Homaeigohar, S.S.; Mahdavi, H.; Elbahri, , M.:

Extraordinarily water permeable sol-gel formed nanocomposite nanofibrous membranes

In: Journal of Colloid and Interface Science (2011) Elsevier

DOI: 10.1016/j.jcis.2011.09.042

Extraordinarily water permeable sol-gel formed nanocomposite nanofibrous membranes

S.Sh. Homaeigohar[a], H. Mahdavi [a,c], M. Elbahri[*a,b]

a: Nanochemistry and Nanoengineering group, Institute of Polymer Research, Helmholtz-Zentrum Geesthacht, Max-Planck-Str. 1, 21502 Geesthacht, Germany

b: Nanochemistry and Nanoengineering group, Institute for Materials Science, Faculty of Engineering, University of Kiel, Kaiserstrasse 2,24143 Kiel, Germany

c: Department of Chemistry, College of Sciences, University of Tehran, Tehran, P.O. Box 14155-6455, Iran

* To whom correspondence should be addressed:

E-mail: mady.elbahri@hzg.de

Tel: +494152872802, Fax: +494152872499

Abstract

Electrospun nanofibrous membranes (ENMs) are considered as a state of the art in water filtration technology mainly owing to their high interconnected porosity and tunable pore size assumed to offer a very high permeability also selectivity. However, the extremely high surface area makes the ENMs prone to mechanical breakdown and lack of wettability lowering the filtration efficiency. Hence, any attempt to enhance both the mechanical properties and hydrophilicity of the ENMs is highly recommended.

In the current study, the structural and transport properties of polyethersulfone (PES) ENMs were modified through incorporation of titania (TiO_2) nanoparticles via a sol-gel approach. Presence of titania precursor increased the conductivity of the electrospun solution thereby optimized the structural features of the electrospun mat in terms of formation of very thin beadless nanofibers, a higher porosity and smaller pore size. Moreover, a significant rise in mechanical properties, thermal stability and switching from a highly hydrophobic membrane to a superhydrophilic one occur simultaneously. The combination of a more optimum porosity, very high mechanical properties and hydrophilicity leads to a significantly higher water permeability in the TiO_2/PES ENMs encouraging us to propose it as a water filtration membrane with longer life span and lower energy consumption.

Keywords: electrospinning, membrane, composite nanofiber, titania nanoparticle, sol-gel

1. Introduction

Nowadays, electrospinning has been recognized as an efficient manufacturing method of nanofibrous structures for a diverse range of applications including filtration [1]. Electrospun nanofibrous mats are highly porous and possess a tunable pore size, thereby extraordinarily permeable and selective, respectively [2-7]. On the other hand, high porosity and surface area of the electrospun nanofibrous membranes make them more exposed to mechanical stresses and depending on the material, hydrophobic interactions leading to clogging the pores and fouling. Therefore, to preserve high permeability and filtration efficiency of such kind of membranes, they should be mechanically reinforced and hydrophilized. The current study's spotlight is on mechanical and wettability modification of the PES ENM to be proposed for water filtration. PES is a well-known membrane material for its high chemical, thermal and mechanical stability however hydrophobic.

In our belief, inorganic nanoparticles can be beneficial in meeting both the mentioned necessities. Inorganic nanoparticles such as titanium dioxide (TiO_2) are inherently hydrophilic and in case of using as a filler can increase the hydrophilicity of the host polymer matrix [8-11]. Moreover, such additives in case of bonding (as hydrogen or covalent i.e. coordination) with polymer functional groups (e.g. ether or sulfone in PES) can hinder chain mobility thereby increase mechanical properties and thermal stability. In a mechanically stable and hydrophilic ENM, porous structure is preserved and water with less resistance passes through the membrane. Such a performance results in a significantly higher permeability, longer life span and lower energy consumption for a nanofibrous membrane.

To fabricate the nanocomposite nanofibrous membrane, sol-gel technique was adopted. This method is based on in-situ generation of inorganic particles in organic phase, including bulk polymer, polymer solutions, and monomer systems [12, 13]. In such an approach the nanoparticles are nucleated and grown inside the host polymer matrix uniformly giving rise to a higher mechanical stability. Moreover, in a nanofibrous structure, the sol-gel formed nanoparticles settle mostly near to and on the surface making them more exposed to the medium thereby maximizing the hydrophilicity.

In the current study, the PES electrospun nanofibers are modified using TiO_2 nanoparticles by a sol–gel process and the properties of the modified PES ENM are characterized by different characterization tests including SEM, TEM, ATR-FTIR, DSC, TGA, water contact angle measurement, porosity and pore size measurement and mechanical tests. To investigate the efficiency of the adopted modification approach on filtration performance i.e. permeability a water flux test was also conducted.

2. Materials and Methods

2.1. Material

Polyethersulfone Ultrason E6020P (M_w= 58,000 g/mol and density of 1.37 g/cm^3) was purchased from BASF (Germany). The solvent *N*,*N*-dimethylacetamide (DMAc) was obtained from Merck (Germany). Trifluoroacetic acid (TFA) and tetra-n-butyl titanate (TBT) (titania precursor) were also obtained from Aldrich chemical co. (USA).

2.2. Preparation of TiO_2 /PES electrospun composite nanofibers

In the current study, PES solution with a concentration of 20 wt% was prepared by dissolving PES flakes in DMAc and acidized with special amount of TFA. Simultaneously, to get titanium precursor sol-solution, TBT was hydrolyzed with TFA for 6 hours at special molar ratio (TFA/TBT) of ≈ 4, then added to PES solution. The amount of TBT was somehow selected to obtain 5 and 8 wt% TiO_2 in the final composite nanofibers. TFA as a catalyst reacts with the alkoxide and forms reasonable complexes which effectively retard hydrolysis during sol synthesis so preventing precipitation [14-16].

The final solution was stirred overnight to obtain a clear homogenous solution for electrospinning. Briefly, for electrospinning the prepared solution was fed with a constant rate of 0.3-0.5 ml/h (depending on the viscosity) into a needle by using a syringe pump (Harvard Apparatus, USA). By applying a 19-23 kV voltage (Heinzinger Electronic GmbH, Germany) electrospinning was done on an Aluminum foil located 25 cm far from tip of the needle for 8 hours. The electrospun nanofibers were left (aged) in air overnight to allow the hydrolysis to go to completion [16].

After electrospinning, in order to in-situ generation of titania nanoparticles a hydrothermal treatment was performed. To do so, the electrospun nanofibers were immersed in a hot water bath (75 °C) for 10 hrs. Through hydrothermal treatment, condensation reaction of the titania precursor occurs and generates TiO_2 nanoparticles [17]. Subsequently, the nanofibers were left to be dried in air overnight. At last, the nanofibrous mat was anealed in oven at 100 °C for 6 hrs to crystallize the amorphous titania formed through sol-gel. The obtained crystalline anatase shows a higher hydrophilicity.

2.3. Morphological characterizations

The morphological characteristics of the electrospun nanofibrous mats in terms of nanofiber diameter and bead formation were investigated through scanning electron microscopy (SEM) (LEO 1550VP Gemini from Carl ZEISS). Moreover, the presence, morphology and distribution mode of the TiO_2 nanoparticles incorporated into the PES electrospun nanofibers were investigated through transmission electron microscopy (TEM) (Tecnai G2 F20 field emission at an acceleration voltage of 200kV). The approximate particle size of the TiO_2 nanoparticles was determined from the SEM images using the Adobe Acrobat v.07 software.

2.4. Surface chemical properties (ATR-FTIR)

Probable bonding of the TiO_2 nanoparticles to PES functional groups was investigated by ATR-FTIR.

Chemical surface analysis of the neat PES and TiO_2/PES electrospun nanofibrous membranes was performed by Fourier Transform Infra Red Spectrometry (FTIR). Attenuated total reflection Fourier transform infrared (ATR-FTIR) spectra were recorded using a Bruker Equinox55 spectrometer.

2.5. Thermal properties (DSC and TGA)

Differential thermal analysis (DSC) and thermal gravitational analysis (TGA) were used to investigate the glass transition (T_g) and thermal decomposition temperature (T_d) of the ENMs.

In DSC measurement (Netzsch DSC 204 Phoenix), the sample was first heated to 300 °C at a speed of 10 °C/min and kept for 5 min under nitrogen atmosphere to eliminate the effect of the thermal history, then the sample was cooled down to 100 °C and the second scan started from 100 °C to 300 °C. The onset of the transition in the heat capacity was defined as glass transition temperature (T_g).

The thermal stability of the neat PES and TiO_2/PES ENMs was evaluated by TGA. Thermal gravimetric analysis (TGA) of the TiO_2/PES ENMs was carried out with a thermogravimetric analyzer of Netzsch 209 TG. TGA analysis was performed at 25–600 ◦C with a heating rate of 10 ◦C/min under Argon. The decomposition temperature (T_d) was defined as the temperature at 5% weight loss.

2.6. Mechanical characterizations

Eventual modification of mechanical properties after addition of TiO_2 nanoparticles to the PES ENMs was evaluated via Dynamic Mechanical Analysis (DMA) and tensile tests as follows:

The frequency-dependant elastic moduli of the neat PES and TiO_2/PES ENMs were measured using a dynamic mechanical analyser (RSA II, Rheometrics Co.) equipped with a tensile fixture. The electrospun nanofibrous samples were cut as 23 mm x 3.9 mm with a thickness of 70 μm. Briefly, frequency-dependent mechanical properties were investigated at the ambient temperature, with a frequency sweep from 0.005 to 100 rad/s using a deformation amplitude of 0.5%.

For tensile test, the neat PES and TiO_2/PES ENMs were carefully cut into rectangular stripes with dimensions of 10 mm x 80 mm and thickness of 60 μm. The tensile properties were characterized by a tensile machine (Zwick/Roell Z020-20KN, Germany) equipped with a 20-N load-cell at ambient temperature. The cross-head speed was 2 mm/min and the gauge length was 20 mm. The reported tensile moduli, tensile strengths and elongations represented average results of 5 tests.

2.7. Water contact angle measurement

Any alteration in wettability of the electrospun membranes owing to addition of TiO_2 nanoparticles was investigated through water contact angle measurement. The static water contact angle of the neat PES and TiO_2/PES electrospun nanofibrous membranes was measured using a contact angle analysis system (Kruess DSA 100, Germany). A 0.5μl droplet was dispensed on the membrane and the resultant angle measured.

2.8. Porosity and pore size measurement

For the porosity measurement, 3 square- shape pieces of the electrospun mats were cut and their area, thickness and mass were accurately measured using a vernier caliper, a digital micrometer (Deltascope ® MP2C from Fischer), an electronic balance (a resolution of 0.1 mg), respectively. The apparent density (ρ) of the electrospun mats were calculated from the obtained mass and the volume. Then the porosity of the electrospun membranes was determined according to the equation (1)[18]:

$$\varepsilon = \frac{(\rho_0 - \rho)}{\rho_0} \times 100\% \qquad (1)$$

Where ε is porosity, ρ_0 and ρ are the average density of the materials used in electrospinning and apparent density of the electrospun mats, respectively. ρ_0 can be calculated according to the equation (2):

$$\frac{1}{\rho_0} = \frac{\phi_{PES}}{\rho_{PES}} + \frac{\phi_{TiO_2}}{\rho_{TiO_2}} \qquad (2)$$

Where ρ_{PES} and ρ_{TiO_2} are 1.37 and 4.23 g/cm^3 , respectively. ϕ_{PES} and ϕ_{TiO_2} are mass fractions of the components.

Subsequently, based on the measured nanofiber diameters (d)(nm) and porosities (ε)(-), the mean pore radius ($\bar{r}$) of the electrospun nanofibrous membranes was calculated according to the equation (3)[19, 20]:

$$\bar{r} = \frac{\sqrt{\pi}}{4}\left(\frac{\pi}{2\log(\frac{1}{\varepsilon})} - 1\right)d \qquad (3)$$

2.9. Water flux measurement

Water flux measurement was performed to see the effect of the applied modifications of the ENMs on their filtration performance. For water flux measurement, circular electrospun membranes, 20 mm in diameter were cut from as-spun nanofiber mats. A custom-built dead-end filtration set-up was designed for the measurements which is shown in Fig. 1. The dried membrane (the active filtration area ≈ 2 cm^2) was placed in the membrane cell and the water in the reservoir (350 ml distilled water) was passed through the membrane cell by applying a feed pressure of 0.5 bar. The time required for permeation of 300 ml water through the membranes was recorded and the flux according to the equation (4) was calculated :

$$J = \frac{Q}{A.\Delta t} \qquad (4)$$

where J is the permeation flux (L/m^2.h), Q is the permeated volume (L) of water, A is the effective area of the membranes (m^2), and Δt is the sampling time (h). The flux measurement tests were repeated three times.

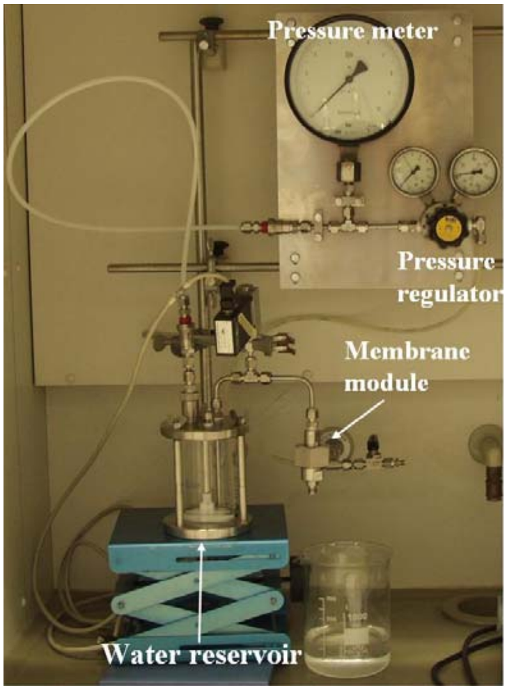

Fig. 1

3. Results and Discussion

3.1. Morphological properties

Morphological characteristics of the electrospun membranes, along with presence, size and distribution mode of titania nanoparticles were investigated by SEM and TEM.

The SEM micrographs of the PES nanofibers with varying TiO_2 contents are illustrated in Fig. 2A. According to the SEM pictures, the measured nanofiber diameters (Fig. 2B) clearly reveal that increase of the amount of TiO_2 results in smaller nanofibers. Moreover, as seen in Fig. 2C, the bead formation is drastically decreased as well. Creation of small beadless nanofibers is attributed to increase of the conductivity of the electrospun solution due to presence of TBT. Such a conductivity rise increases electrical repulsion force i.e. bending instability stretching the jet and lowers the surface tension induced bead formation considerably [1].

Furthermore, judged by the SEM micrographs, the TiO_2 nanoparticles with a size around 24 ± 8 nm are well dispersed in both the compositions on the surface of the nanofibers. As seen in Fig. 2D, such finding is confirmed by TEM pictures as well. The TEM images clearly reveal homogenous distribution of the nanoparticles inside and mostly near/on to the surface of the nanofibers which can be important in terms of mechanical property and hydrophilicity, respectively. The interior nanoparticles are formed when a minor part of the TBT is converted to TiO_2 nanoparticles while preparation of the solution to be electrospun or even while the electrospinning. Such nanoparticles owing to an acidic environment caused by TFA, are highly protonated and positively charged [21]. On the other hand, the solution jet ejected from the needle connected to the positive electrode of high-voltage power supply is highly charged. The positive charges accumulating on the outer surface of the electrospinning jet are able to repel the positive charged TiO_2 nanoparticles to the middle of the nanofibers being formed. Moreover, evaporation of the solvent from the surface of the jet is compensated with the interior solvent. The dissolved TBT is transferred toward the surface of the jet by such an outward flow[22] and is converted to the titania nanoparticles on or near to the surface of the nanofibers. The concomitant uniform dispersion of the very fine nanoparticles inside and onto the nanofibers is generic to our approach and could be due to the eventual chemical bond between the TiO_2 nanoparticles and the sulfone (or ether) functional group of PES. This behaviour can be probed by ATR-FTIR.

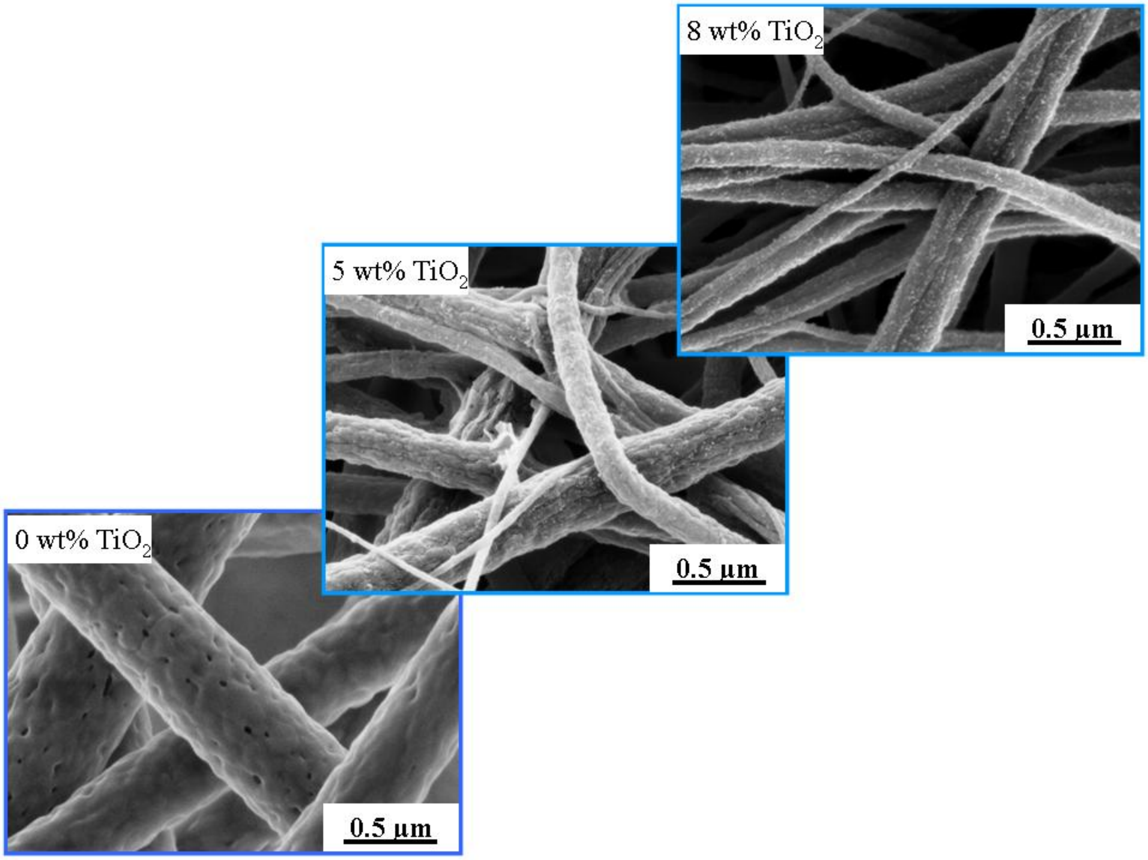

(A)

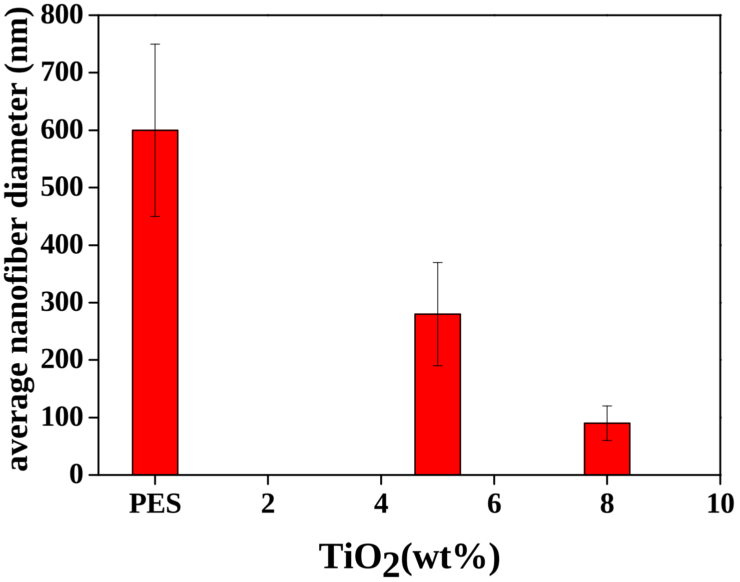
average nanofiber diameter (nm)
0
100
200
300
400
500
600
700
800
PES
2
4
6
8
10
TiO2(wt%)

(B)

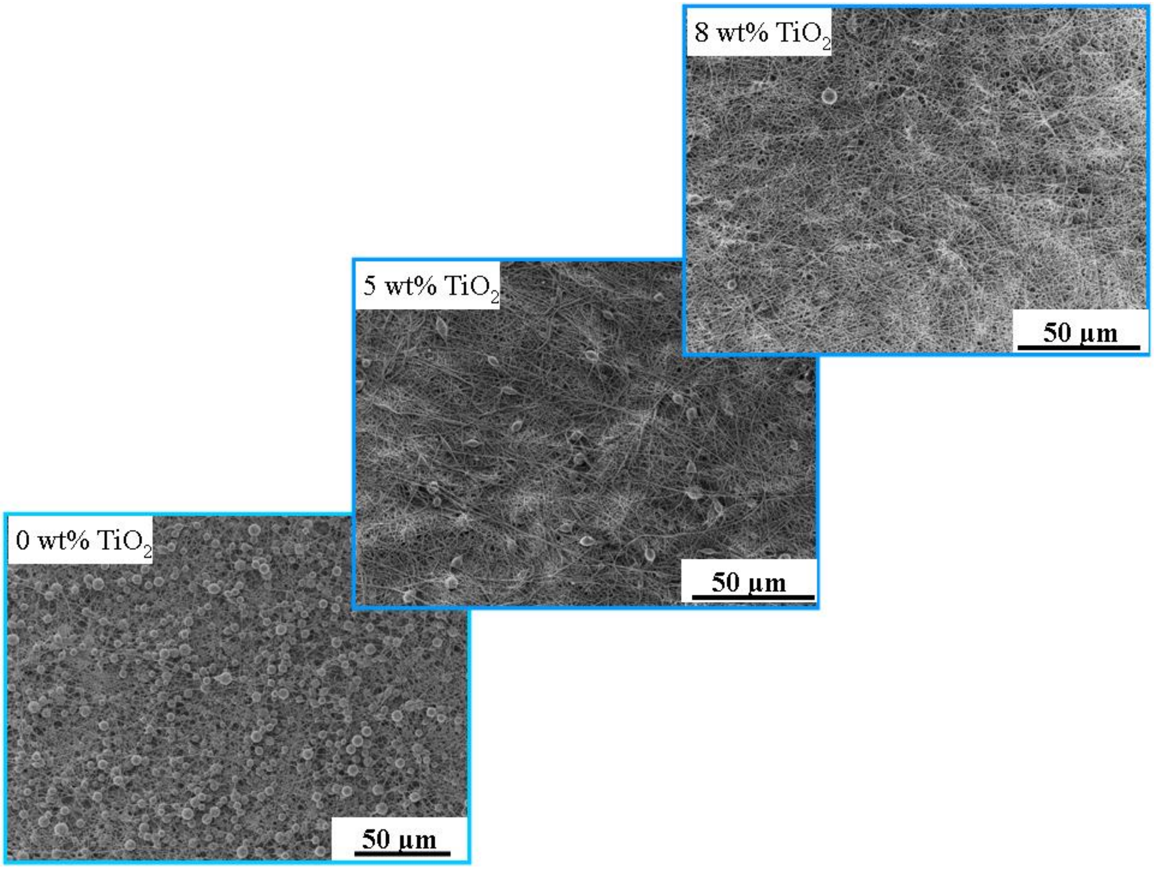
8 wt% TiO2
50 µm
5 wt% TiO2
50 µm
0 wt% TiO2
50 µm

(C)

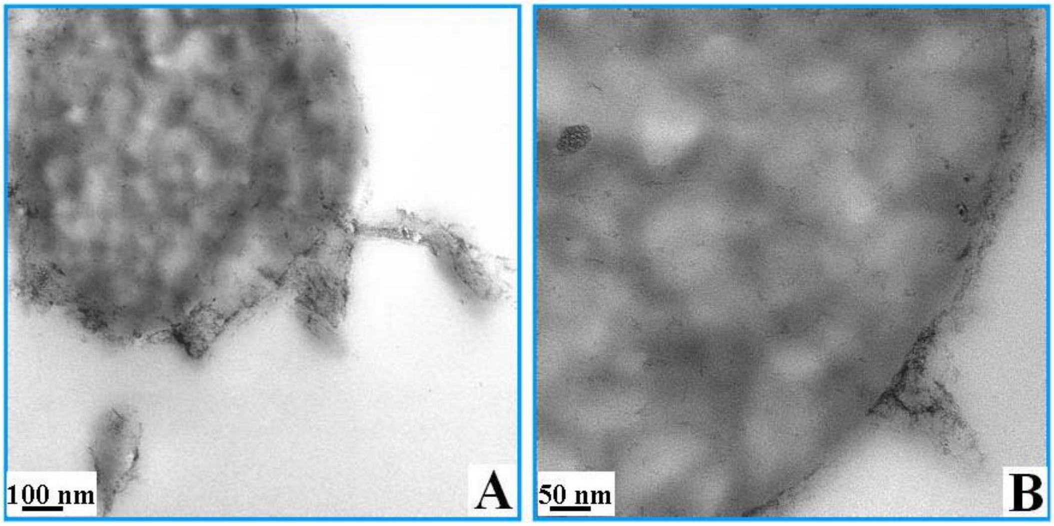

(D)

Fig.2

3.2. Surface chemical properties (ATR-FTIR)

The general features of the ATR-FTIR spectra of the neat PES and the TiO_2/PES composite ENMs with different TiO_2 content are shown in Fig. 3. The absorption peaks at 1296 and 1146 cm^{-1} attribute to the asymmetrical and symmetrical vibrations of the sulfone group, respectively. The absorption peak at 1234 cm^{-1} attributes to the stretching vibration of the ether C-O-C bond in the PES polymer [23]. A comparison between the ATR-FTIR spectra of the neat and composite ENMs reveal that the position of the peak at 1234 cm^{-1} for the neat PES ENM shift to 1239 and 1241 cm^{-1} for the TiO_2/PES composite ENMs with 5 and 8 wt% TiO_2, respectively. This shift is due to the in situ formation of TiO_2 nanoparticles in the PES matrix [8]. While the hydrolysis and condensation of TBT form into TiO_2 sol, partially cross-linking reactions happen due to hydrogen bonding interaction between the Ti-OH or Ti-$OCH_2CH_2CH_2CH_3$ and ether C-O-C bond (or sulfone SO_2 group) [8]. Such bonding shifts the peak related to the bonded functional group. The bonding between the TiO_2 nanoparticles and the functional groups of PES could lead to a more optimum thermal and mechanical stability.

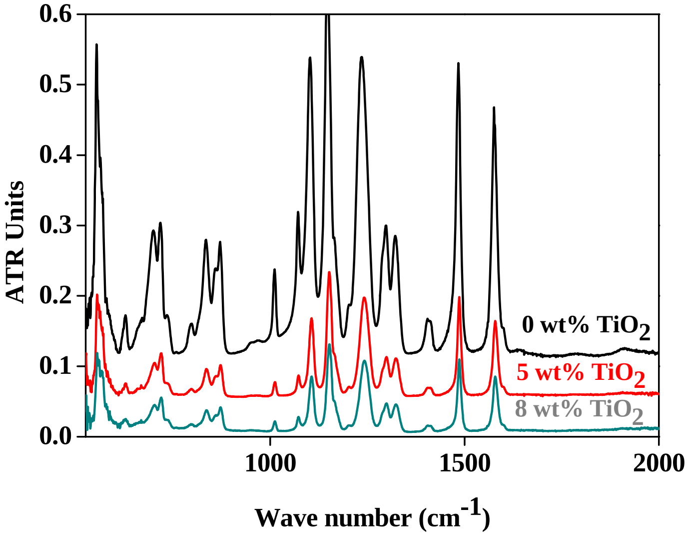

Fig. 3

3.3. Thermal properties

The DSC and TGA results shown in Fig. 4, clearly reveal that the glass transition temperature (T_g) and thermal decomposition temperature (T_d) of the membranes are increasing with increase of the amount of TiO_2 most probably due to the interactions between TiO_2 nanoparticles and the polymer [17, 24, 25]. The interaction between TiO_2 nanoparticles and PES as a hydrogen bond between the surface hydroxyl group and the sulfone or ether group of PES increases the rigidity of polymer chain and enhances the energy of breaking down the polymer chain [24]. On the other hand, with increasing of TiO_2 content, more heat is absorbed by the TiO_2 in the membranes during heating-up, the decomposition of PES is thus delayed, and the decomposition temperature of TiO_2/PES ENMs is enhanced [26].

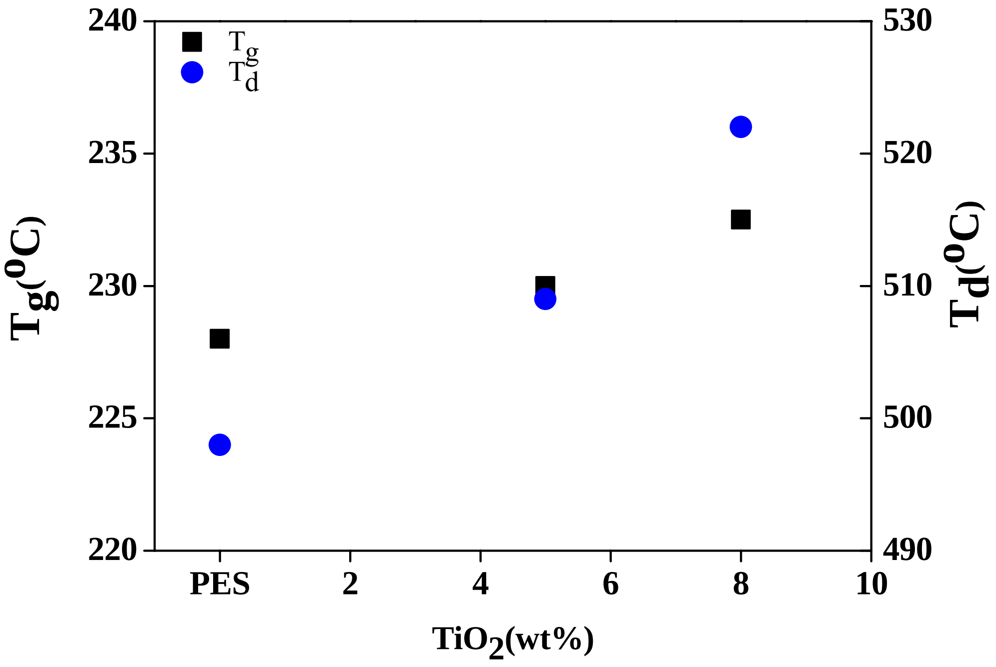

Fig. 4

3.4. Mechanical properties

In addition to thermal stability, bonding of the nanoparticles to the polymer chains could lead to a higher mechanical properties in the PES ENMs. In fact, a more stable nanoparticle-polymer interface could lead to a more efficient load transfer thereby a higher mechanical properties [27-29]. As shown in Fig. 5A, the dynamic storage modulus (E') of the TiO_2/PES composite ENMs obtained by DMA measurements is much higher than that of the neat PES ENM. The TiO_2/PES ENM containing 5 wt% titania show the highest storage modulus while at 8 wt% , E' declines but still remains two times higher than that of the neat PES ENM.

Tensile test results are also demonstrated as Fig. 5B. Similar to the DMA results, elastic modulus and tensile strength increase significantly with addition of titania especially with a higher rate for the TiO_2/PES ENM containing 5 wt% titania.

As explained before, TiO_2 nanoparticles can act as a cross linking point to link the polymer chains and increase their rigidity. So there is a need to more energy to beak down the bond between nanoparticles and PES chains and the mechanical properties of the composite ENMs are improved [24]. Reduction of the increase rate of mechanical properties after the concentration of 5 wt%, can be attributed to the following reasons:1) slight agglomeration which lowers the surface area of the nanoparticles and interfacial interaction between TiO_2 and PES 2) increase of the free volume of the polymer matrix around the TiO_2 nanoparticles and subsequent decrease of the mechanical properties [8].

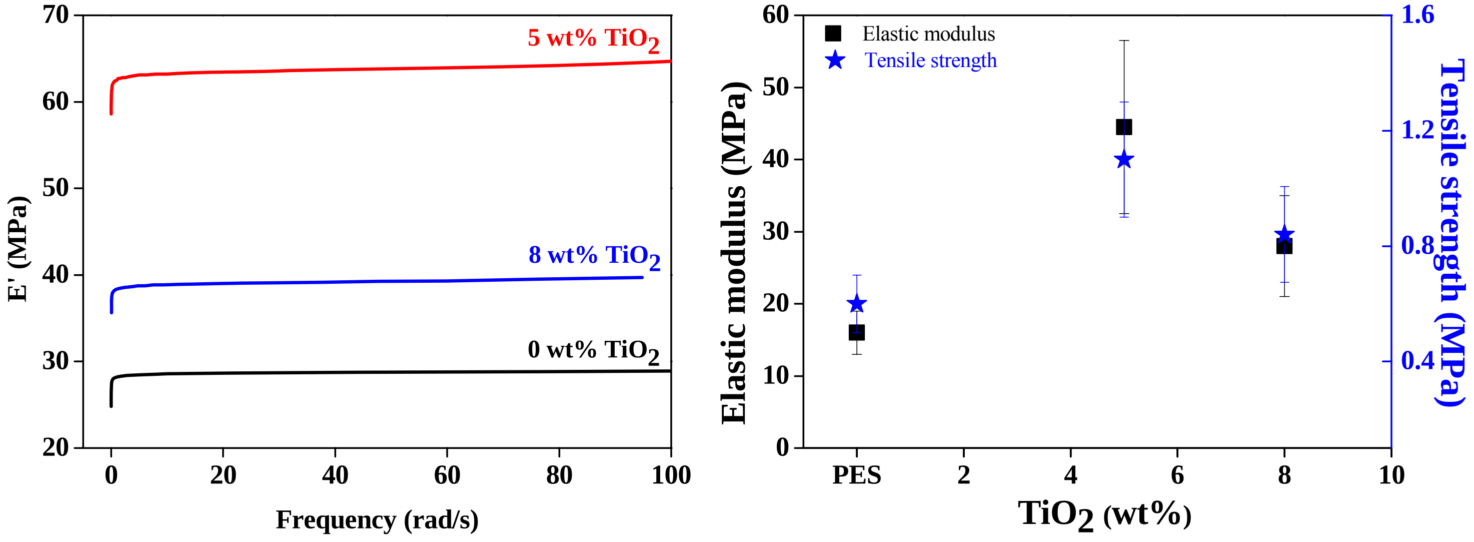

(A) (B)

Fig. 5

3.5. Hydrophilicity

While the interior TiO_2 nanoparticles contribute mainly to enhancement of the mechanical properties and thermal stability, those mounted on the surface can also induce an extraordinary hydrophilicity to the nanofibers. According to the TEM observations (Fig. 2D) it is seen that the nanoparticles mostly settle on or near to the surface of the nanofibers. This mode of distribution of the TiO_2 nanoparticles makes them more exposed to the medium optimizing the interaction of the nanofibers with water molecules and as shown in Fig. 6 enhancing hydrophilicity of the ENMs. This property is quite promising especially for water filtration application to minimize fouling [30] and filtration resistance.

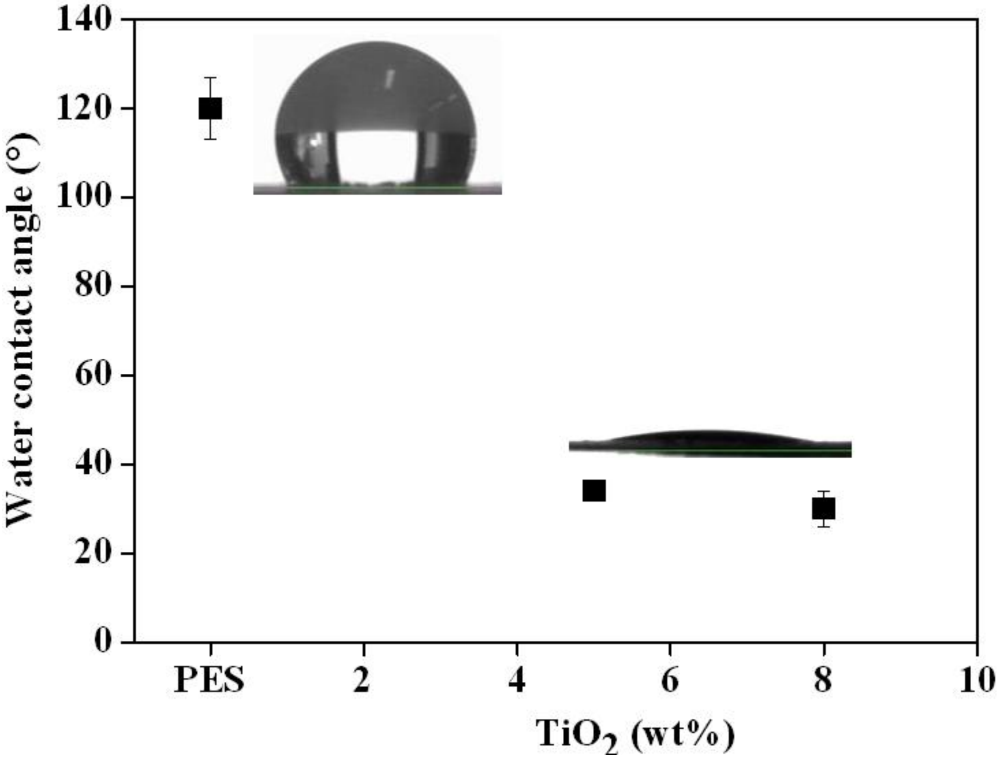

Fig. 6

3.6. Porosity and pore size

Formation of the smaller beadless composite nanofibers as seen in Figs. 2 A-C could lead to a significant change in the porous structure of the membranes. As shown in

Fig. 7, addition of the TiO_2 nanoparticles results in a higher porosity and smaller pore size primarily owing to the less bead formation and smaller fiber diameters, respectively. The most optimum structure is observed at the highest TiO_2 concentration i.e. 8wt% possessing the highest porosity and smallest pore size thereby the highest permeability and size selectivity.

Interestingly, while the PES ENM shows the lowest porosity and according to the equation (5) is expected to show the highest mechanical properties, the composite ENMs possess a more mechanical stability.

The effective elastic modulus for a highly porous structure such as an electrospun nanofibrous membrane can be expressed by equation (5)[31, 32] :

$$E = E_m(1-\phi)^2 \qquad (5)$$

Where E and E_m stand for the effective elastic modulus of the porous (with porosity of ϕ) and bulk material, respectively.

The reasons could be the smaller nanofibers eventually possessing a higher chain alignment [33] also the nanoparticles which physically cross link the polymer chains.

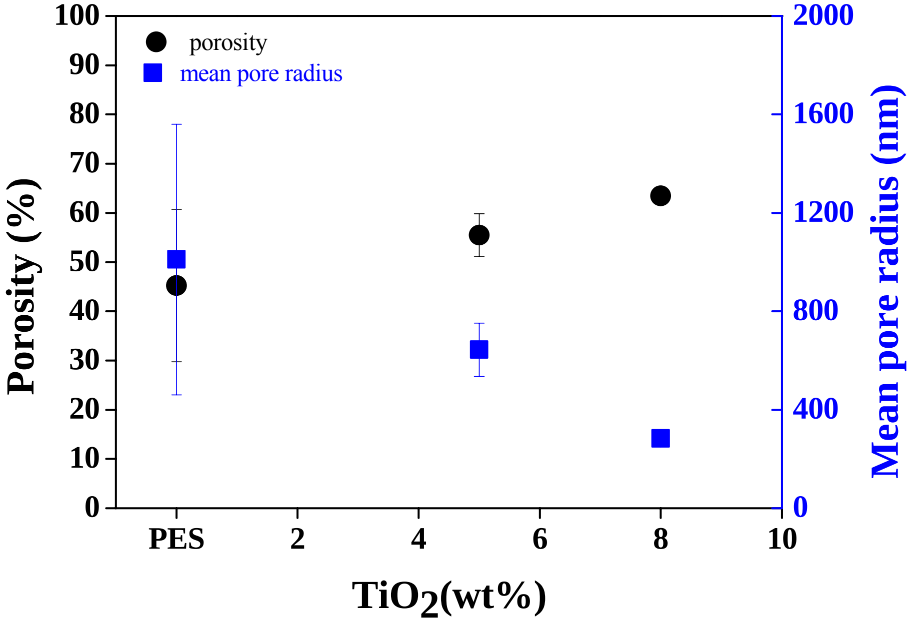

Fig. 7

3.7. Water permeability

The main goal sought after addition of titania nanoparticles to the PES ENMs is improvement of water permeability of the membranes through their structural, mechanical and surface chemical improvements.

Water flux behavior of the TiO_2/PES composite ENMs is presented as Fig. 8. Addition of titania nanoparticles increases the water permeability of the membranes significantly. This enhancement is due to several factors including the higher porosity, mechanical stability as well as hydrophilicity of the composite ENMs. Mechanically stable ENMs can preserve their intact porous structure while filtration. In addition, high hydrophilicity leads to a lower resistance to water flow passing through the membrane. Such promising combination offers a really high permeability which lengthen the life span and lowers energy consumption of a water filtration process.

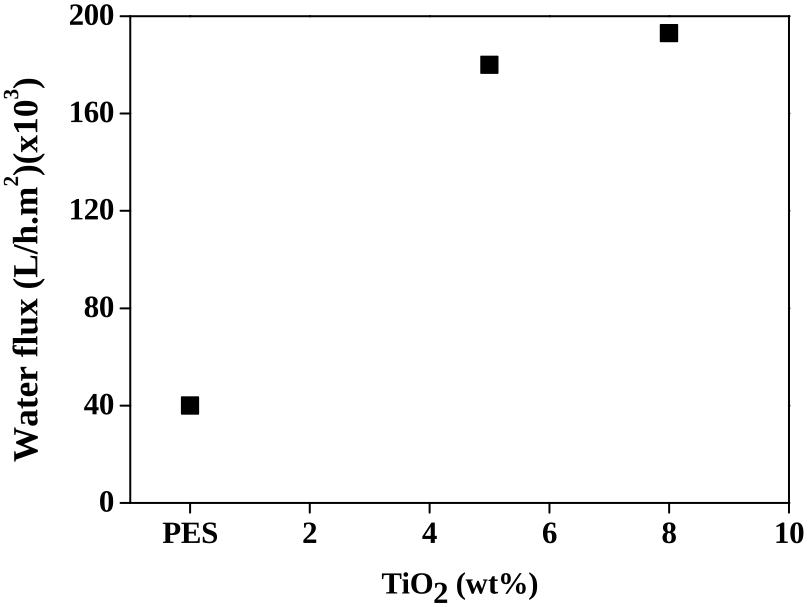

Fig. 8

4. Conclusion

While promising properties such as high interconnected porosity and tunable pore size tempt researchers to evaluate electrospun nanofibrous membranes for filtration applications, low wettability and mechanical stability seems as two main obstacles ahead. The latter deficiency minimizes the porosity while filtration thereby permeability, while the former one increases fouling tendency and filtration resistance.

In our study, we showed that incorporation of highly hydrophilic titania nanoparticles into PES nanofibers maximizes wettability and mechanical stability thereby permeability of the relevant ENMs. Extraordinary exposure of titania nanoparticles formed on the surface of nanofibers to the medium due to sol-gel technique and their bonding to PES chains are responsible for the high hydrophilicity and mechanical stability, respectively. High obtained permeance is interpreted as lower energy consumption and longer life span of this novel class of water membranes.

Acknowledegement

The first author would like to appreciate the financial support from a Helmholtz-DAAD PhD fellowship. Clarissa Abetz for TEM and Karen Prause for SEM pictures, and Heinrich Böttcher for tensile tests and DMA are gratefully acknowledged.

References

[1] Z.M. Huang, Y.Z. Zhang, M. Kotaki, S. Ramakrishna, Comp. Sci. and Tech. 63 (2003) 2223.

[2] Z. Tang, C. Qiu, J.R. McCutcheon, K. Yoon, H. Ma, D. Fang, E. Lee, C. Kopp, B.S. Hsiao, B. Chu, J. Polym. Sci. Part B: Polym. Phys. 47 (2009) 2288.

[3] P. Heikkila, A. Taipale, M. Lehtimaki, A. Harlin, Polym. Eng. Sci. 48 (2008) 1168.

[4] K. Nakata, S.H. Kim, Y. Ohkoshi, Y. Gotoh, M. Nagura, Sen-I Gak. 63 (2007) 307.

[5] X.H. Qin, S. Wang, J. Appl. Polym. Sci. 102 (2006) 1285.

[6] W.J. Li, C.T. Laurencin, E.J. Caterson, R.S. Tuan, F. Ko, J. Biomed. Mater. Res. 60 (2002)613.

[7] C. Burger, B.S. Hsiao, B. Chu, Annu. Rev. Mater. Res. 36 (2006) 333.

[8] M.L. Luo, W. Tang, J.Q. Zhao, C. Pu, J. Mater. Process. Tech. 172 (2006) 431.

[9] T. Matsuura, Y. Taketani, S. Sourirajan, Ind. Eng. Chem. Process Des. Dev. 95 (1983) 10.

[10] A. Fujishima, K. Honda, Nature 238 (1972) 37.

[11] A.L. Linsebiger, G.Q. Lu, T. John, Chem. Rev. 95 (1995) 735.

[12] T. Kyprianidou-Leodidou, P. Margraf, W. Caseri, U. Suter., P. Walther, Polym. Adv. Technol. 8 (1997) 505.

[13] Mikrajuddin, I.W. Lenggoro, K. Okuyama, F. Shi, J. Electrochem. Soc. 149 (2002) 107.

[14] P. Viswanathamurthi, N. Bhattarai, H.Y. Kim, D.R. Lee, S.R. Kim, M. Morris, Chem. Phys. Lett. 374 (2003) 79.

[15] O. Carp, C.L. Huisman, A. Reller, Prog. in Solid State Chem. 32 (2004) 33.

[16] D. Li, Y. Xia, Nano Lett. 3 (2003) 555.

[17] X. Meng, N. Luo, S. Cao, S. Zhang, M. Yang, X. Hu, Mater. Lett. 63 (2009) 1401.

[18] H. Na, Y. Zhao, X. Liu, C. Zhao, X. Yuan, J. Appl. Polym. Sci.122 (2011) 774.

[19] S.J. Eichhorn, W. Sampson, J.R. Soc. Interf. 2 (2005) 309.

[20] W. Sampson, J. Mater. Sci. 38 (2003) 1617.

[21] Q. Hu, E. Marand, Polymer 40 (1999) 4833.

[22] R.D. Deegan, O. Bakajin, TF. Dupont, G. Huber, SR. Nagel, T. Witten, Nature 389 (1997) 827.

[23] S. Belfer, R. Fainchtain, Y. Purinson, O. Kedem, J. Membr. Sci. 172 (2000) 113.

[24] J.F. Li, Z.L. Xu, H. Yang, L.Y. Yu, M. Liu, Appl. Surf. Sci. 255 (2009) 4725.

[25] T. H. Bae, I. C. Kim, T. M. Tak, J. Membr. Sci. 275 (2006) 1.

[26] G. P. Wu, S. Y. Gan, L. Z. Cui, Y. Y. Xu, Appl. Surf. Sci. 254 (2008) 7080.

[27] R. Roger (Ed.) Particulate-filled Polymer Composites, Rapra Technology Limited, Shrewsbury, 2003.

[28] S.SH. Homaeigohar, A. Yari Sadi, J. Javadpour, A. Khavandi, J. Euro. Cer. Soc. 26 (2006) 273.

[29] G. Carotenuto, M. Valente, G. Sciume, T. Valente, G. Pepe, A. Ruotolo, L. Nicolais, J. Mater. Sci. 41 (2006) 5587.

[30] R. Baker, Membrane technology and applications, Wiley, 2004.

[31] G. Lu, G.Q. Lu, Z. Xiao, J. Por. Mater. 6 (1999) 359.

[32] R. Pal, J. Comp. Mater. 39 (2005) 1147.

[33] Z. Chen, B. Wei, X. Mo, C.T. Lim, S. Ramakrishna, F. Cui, Mater. Sci. and Eng;C 29 (2009) 2428.

Figure captions:

Fig. 1. Permeation set-up used for the water flux measurements

Fig. 2. A) SEM micrographs of the TiO_2/PES electrospun nanofibers B) Average diameter of the TiO_2/PES electrospun nanofibers C) Drastical decrease of bead density with amount of TiO_2 nanoparticles D) TEM pictures showing the TiO_2 nanoparticles (8 wt%) distributed in cross- section of the nanofibers

Fig. 3. ATR-FTIR spectra of the neat PES ENM versus TiO_2/PES ENMs

Fig. 4. Thermal properties of the TiO_2 / PES electrospun nanofibrous membranes

Fig. 5. Mechanical properties of the TiO_2 / PES electrospun nanofibrous membranes according to A) DMA B) tensile test

Fig. 6. Water contact angle measured for the neat and TiO_2 /PES electrospun nanofibrous mats

Fig. 7. Porosity and pore size measurement of the TiO_2 / PES electrospun nanofibrous membranes

Fig. 8. Water flux measured for the neat and TiO_2 /PES electrospun nanofibrous mats